High-Definition Mapping of the Gutenberg-Richter *b*-value and its Relevance: a Case Study in Italy

Matteo Taroni[1], Jiancang Zhuang[2] and Warner Marzocchi[3]

[1] Istituto Nazionale di Geofisica e Vulcanologia, Rome, Italy

[2] The Institute of Statistical Mathematics, Tokyo, Japan

[3] University of Naples, Federico II, Dept. of Earth, Environmental, and Resources Sciences, Naples, Italy

Corresponding author:

Matteo Taroni, address: Via di Vigna Murata 605, 00143, Rome, RM, Italy; email: matteo.taroni@ingv.it

Declaration of Competing Interests:

The authors acknowledge there are no conflicts of interest recorded

ABSTRACT

The spatial variability of the magnitude-frequency distribution is important to improve earthquake forecasting capabilities at different time scales. Here, we develop a novel approach, based on the weighted maximum likelihood estimation, to build a spatial model for the *b*-value parameter of the Gutenberg-Richter law and its uncertainty, also for earthquake catalogs with a time-varying completeness magnitude. Then, we also provide a guideline based on the Bayes factor to measure the importance of the *b*-value spatial variability with respect to a model having a spatially uniform *b*-value. Finally, we apply the procedure to a new Italian instrumental earthquake catalog from 1960 to 2019 to investigate the *b*-value spatial variability over the Italian territory.

INTRODUCTION

The size distribution of the earthquakes is commonly described by the Gutenberg-Richter law (Gutenberg and Richter, 1944):

$$log_{10}N(M) = a - bM \qquad (1)$$

where $N(M)$ is the cumulative number of earthquakes with magnitude $\geq M$, *a* is the "productivity" parameter (10^a represents the total number of events with magnitude ≥ 0) and *b* is the so-called *b*-value. The *b*-value rules the relative size distribution of the earthquakes, i.e. the percentage of larger events with respect to the smaller ones. Although different methods are available (Bender, 1983; Castellaro et al., 2006), the most common approach is the maximum likelihood method (Aki, 1965), with some additional correction for potential biases (Marzocchi et al., 2020).

Estimation of the *b*-value in many earthquake catalogs shows a *b*-value=1 (Kagan and Jackson, 2000); however, selecting the earthquakes according to some peculiar property (e.g. the focal mechanism) or in some particular zones (such as in volcanic areas), is possible to observe departures from the universal value 1. Many studies suggest that the *b*-value is correlated with the differential stress in the earth's crust: the smaller the *b*-value, the larger the differential stress (Scholz, 1968; Schorlemmer et al., 2005). This correlation implicitly implies that the *b*-value varies across different styles of faulting, leading to larger *b*-values for normal faulting and smaller *b*-values for inverse faulting (Schorlemmer et al., 2005; Gulia and Wiemer, 2010).

A common method to identify the spatial heterogeneity of the *b*-value is the mapping of this parameter; such maps are obtained by dividing earthquake catalogs in convenient ways. For example, using geological and/or seismotectonic considerations to define spatially homogeneous regions with earthquakes having similar properties, such as similar focal mechanisms (Gulia and Wiemer, 2010) or style of faulting (Meletti et al., 2008). Another approach is to define a uniform spatial grid, and then for each point of this grid compute the *b*-value using only earthquakes within a predefined distance; this approach can be useful both for mapping the *b*-value along a fault (Schorlemmer et al., 2004) and for the mapping of a wider area (Tormann et al., 2014; Tormann et al., 2015). To our knowledge, the first attempt to introduce a weighting scheme in the estimation of the *b*-value was made by Tormann et al. (2014), assigning a distance-dependent weight to each earthquake. This paper is pioneering regarding the weighting spatial *b*-value mapping, however, it does not offer a technical statistical framework for the estimation method, and in particular for the uncertainty computation.

Once estimated the spatial distribution of the *b*-value, the most challenging aspect is to quantify how much the apparent *b*-value spatial variability improves the forecast of a model based on a single *b*-value (Hiemer and Kamer, 2016). Eventually, this information has to be carefully evaluated to figure out the motivations of possible variations. In fact, it is well known that many of the *b*-value variations are caused by non-physical factors (Kamer and Hiemer, 2015; Marzocchi et al., 2020; Herrmann and Marzocchi, 2021).

The goal of this paper is to create a statistical framework where it is possible to estimate, using some weighting scheme, both the *b*-value and its uncertainty. The weighted likelihood approach (Hu and Zidek, 2002), which has been already applied in other seismic spatial estimation distribution problems (Zhuang, 2015), is probably the best way to introduce a weighting scheme maintaining a formally correct statistical approach. To illustrate the application of the method, and how to estimate the statistical significance of the *b*-value spatial variability, we apply the procedure to the Italian instrumental catalog (Lolli et al., 2020) from 1960 to 2019, with a completeness magnitude that varies with time.

METHODS

Weighted maximum likelihood estimation for the *b*-value and its uncertainty

The classical maximum likelihood estimation (MLE) for the *b*-value of the Gutenberg-Richter law (Aki, 1965), considering the correction for the binning of the magnitudes (Utsu, 1966), leads to the equation:

$$\hat{b} = \frac{1}{\ln(10)\left(\bar{M} - \left(M_{min} - \frac{\Delta M}{2}\right)\right)} \qquad (2)$$

where $\bar{M}$ is the mean of the magnitudes in the catalog, M_{min} is the completeness magnitude of the catalog and ΔM is the binning of the magnitude (usually 0.01 for Mw and 0.1 for Ml). Here we use $\hat{b}$, whose value depends on the observations, to denote our estimate of the true *b*-value, whose exact value is unknown value. In the case of catalogs with a completeness magnitude that varies with time, i.e. the minimum magnitude depends on the *k*-th time window considered $M_{min}^{(k)}$, Taroni (2021) shows that eq. (2) became:

$$\hat{b} = \frac{1}{\left(\frac{\sum_{i=1}^{N}\left(M_i - M_{min}^{(k)}\right)}{N} + \frac{\Delta M}{2}\right)\ln(10)} \qquad (3)$$

where N is the total number of events in the catalog, and $M_{min}^{(k)}$ is the k-th threshold of completeness relative to the i-th earthquake with magnitude M_i(see Fig. 1 in Taroni 2021). Using the weighted MLE (Hu and Zidek, 2002), if we assign to each event a positive weight W_i , where the sum of all the W_i is 1, equation (3) can be generalized as:

$$\hat{b} = \frac{1}{\left(\sum_{i=1}^{N} W_i\left(M_i - M_{min}^{(k)}\right) + \frac{\Delta M}{2}\right)\ln(10)} \qquad (4)$$

see Appendix A for more details on this equation. The MLE of the sample standard deviation $\sigma_{\hat{b}}$, that represents the uncertainty on $\hat{b}$, described by Aki (1965), can also be generalized in the weighted MLE context with:

$$\hat{\sigma}_{\hat{b}} = \hat{b}\sqrt{\sum_{i=1}^{N} W_i^2} \qquad (5)$$

by applying the delta method (Dorfman, 1938; see Appendix B for details).

Once defined the equations useful to estimate the *b*-value and its uncertainty, we can describe the kernel used for the spatial estimation. In this work, we adopt a Gaussian kernel, widely used in seismic parameters estimation (Frankel, 1995), depending on the distance R of the i-th earthquake from the considered spatial point; then $W_i \propto \exp\left(-\frac{R^2}{2d^2}\right)$, where d is the smoothing distance (Helmstetter et al., 2007). Obviously, if we put all weights equal to $1/N$, the equations of weighted MLE became equivalent to the classical MLE.

This approach has a clear advantage with respect to the classical approach based on one fixed radius search. The former does not have a hard boundary like the latter, where all the events within the selected radius have weight 1 and all the others 0; using a smoothing kernel we can gradually decrease the importance of the observation with the distance. The final result is a *b*-value estimation coherent with the hypothesis that this parameter can continuously change along different zones (Tormann et al., 2014).

Quantifying the importance of the *b*-value variations

To test the statistical significance of the *b*-value variations observed, we compare the log-likelihood of a model that considers the spatial variability of the *b*-value (model A), and a model based on one single common *b*-value over the whole region (model B). The log-likelihoods are calculated using independent observations contained in a testing catalog, which have not been used to calibrate the model (pseudo-prospective test). The log-likelihood of model A given a set of observations $Obs = \{X_1, \dots, X_M\}$ is defined by:

$$LL_A = \sum_{i=1}^{N_T} \ln f_A(X_i) \qquad (6)$$

where N_T is the total number of events in the testing catalog, f_A is the probability density function of model A and $X_i = M_i - M_{min}$, with M_i the magnitude of the i-th event and M_{min} the completeness magnitude of the testing catalog (Kamer and Hiemer, 2015). The function f_A can vary in each spatial cell, depending on model A. The model B is built in the same way as equation (6), but f_B has the same *b*-value for the whole region. Since we use a testing catalog composed of observations independent from the one used to estimate the parameters of the models, the difference between the log-likelihoods resembles numerically the log Bayes factor (Eq. 4 in Marzocchi et al., 2012). Hence, though the Bayes factor was implemented in a different context (Kass and Raftery, 1995), we can adopt the Bayes factor terminology (see Table 2 in Kass and Raftery, 1995) to describe to what extent the model with the spatial varying *b*-value is better than the model with a uniform *b*-value.

DATA FROM THE ITALIAN INSTRUMENTAL SEISMICITY

In this work, we apply our methodology to the Italian instrumental seismic catalog of Lolli et al. (2020) from 1960 to 2019 (see Data and Resources), taking from granted the information of the completeness magnitude given for this catalog (see Table 1).

We select the events with a depth ≤ 30 Km, with magnitudes above the completeness magnitude, and inside a polygon that excludes the zones far on the sea (see Fig. 1), where the completeness magnitudes can be different from the inland zones (Lolli et al., 2020). To avoid the short-term incompleteness induced by strong events (Kagan, 2004; Lolli and Gasperini, 2006), after an Mw 5.5 or greater earthquake we remove all the events within 3 days and 30 Km from the epicenter of the shock. This final catalog contains 56,309 events.

b-VALUE MAPPING AND MODEL COMPARISON FOR ITALY

b-value mapping

We estimate the *b*-value using the weighted MLE over the 0.1°x0.1° spatial grid inside the study region, using a Gaussian kernel with a smoothing distance of 30 Km; this distance was already used in the Italian region (Murru et al., 2016), and it is a distance suitable to identify possible departures from the uniform *b*-value due to local crustal properties (e.g. characteristic fault mechanism). In the Supplemental Material, we also perform the same computation for 20, 25, 35, and 40 Km, and for a conservative completeness magnitude (adding 0.2 to all the completeness magnitudes in Table 1) obtaining very similar results. To avoid confusion, we use *b*-$\hat{b}$ for the spatial varying *b*-value as a function of locations, and *B*-$\hat{B}$ for the constant *B*-value of the whole catalog. Together with the *b*-value, we also estimate the sample standard deviation $\sigma_{\hat{b}}$. Approximating the confidence interval (CI) of the estimated *b*-value with the Gaussian distribution (Aki, 1965), we also compute the 95% CI as $[\hat{b} - 1.96\,\hat{\sigma}_{\hat{b}}; \hat{b} + 1.96\,\hat{\sigma}_{\hat{b}}]$ in each spatial cell. Then we map the *b*-values only in the spatial cells where the *B*-value computed for the whole catalog ($\hat{B} = 1.04$) fall outside the 95% CI of the *b*-value computed for the spatial cell. This very simple but innovative representation is quite useful because allows showing only the *b*-values that are significantly different from one of the whole catalog (here the word "significantly" is related to the computed 95% CI, and is not used as the result of a statistical test).

In Fig. 2 we show three different types of maps: in panel (a) we show the *b*-value map, in panel (b) the standard deviation, and in panel (c) the *b*-values significantly different from the one of the whole catalog.

The first map (Fig. 2a) shows a lot of zones with low/high *b*-values, but some of these zones are the same with high values of standard deviation. In fact, it's easy to have a large deviation from the *B*-value of the whole catalog where we have few events: for this reason, the most important map is the third one (Fig. 2c), which combines both *b*-value and his standard deviation to show only the zones with a *b*-value significantly different from 1.04.

This third map (Fig. 2c) shows some zones with a high *b*-value and some other zones with a low *b*-value. Remarkably, Marzocchi et al. (2020) show that the completeness magnitude for the whole catalog may not hold locally, and this can induce severe biases in the *b*-value. In particular, this work shows that if a portion of the catalog is affected by local incompleteness, the corresponding b-value is usually lower than the overall value. Specifically, Schorlemmer et al. (2010) show that the existing seismic network in the Italian region has a strong inhomogeneity leading to spatial variability of the network detection capability. That study shows a low detection capability (higher completeness magnitude) in the Southern part of Apulia, the Western part of Sicily, and the North-East near the border with Austria; then, the low *b*-value evidenced in these zones can be explained by the use of the same common completeness magnitude in the whole Italian region. The high *b*-values in the central Apennines, Northern part of Apulia, and Western part of Tuscany are more interesting, and can be due either to the prevalent normal faulting of these zones (in particular for the central Apennines, Gulia and Wiemer, 2010), or, higher heat flux (in particular for Tuscany, Della Vedova et al., 2001) which may lead to high b-values (Warren and Latham, 1970).

Quantifying the importance of the spatial *b*-value variations for Italy

To compare the performance of the model with a uniform *B*-value and the model with a spatial-varying *b*-value, we implement a pseudo-prospective test. We use the data from 1960 to 2009 to build the two models and then a testing dataset from 2010 to 2019 to compute the Bayes factor (BF) from the log-likelihoods of the model (according to eq. (6)). In Fig. 3 we show the cumulative Bayes factor (in a log scale) for three different completeness magnitudes 1.8, 2.1, and 2.4. Along with the Bayes factor curves, we also show the “very strong evidence” line (Table 2 in Kass and Raftery, 1995): if the Bayes factor curve is above this line, it brings very strong evidence in favor of the model with a spatial-varying *b*-value against the model with a uniform *B*-value. Since the figure shows the cumulative Bayes factor, the final results of the comparison correspond to the last day of the test (i.e. in the right part of the figure, around day 3650).

Fig. 3 shows a generally better performance of the model with a spatial-varying b-value, independently from the completeness magnitude chosen for the testing catalog. Increasing the overall completeness magnitude, the evidence in favor of the model based on the b-value spatial variability tends to decrease; this may be due to the fact a higher overall completeness magnitude reduces the advantage of the model in regions that have a local completeness magnitude lower than the overall one (because we reduce the number of events in the testing catalog). During the 2016 Amatrice-Norcia sequence, around the 2500th day, we observe the strongest increase of the Bayes factor. The great performance of the spatial-varying model during this sequence is probably due to the high b-value forecasted by such a model (with respect to the uniform model) in the central Apennines zone, where this sequence took place. This great performance can also be influenced by a possible temporary high b-value induced by strong events of the sequence (Gulia et al., 2018).

A deeper interpretation of these results is beyond the scope of this paper which aims at showing the benefits of the approach to detect *b*-value spatial variations and to quantify the importance of such variations.

LIMITATIONS AND FURTHER IMPROVEMENTS

For our computations, we have assumed an exponential distribution of the magnitudes (i.e. a Gutenberg-Richter law): if this assumption is not satisfied by the data, our method (as well as any other method to calculate the *b*-value) can lead to biased results.

Our methodology can be greatly improved by using a detailed computation of the magnitude of completeness, that can vary both with space and time (Tormann et al., 2014). In particular, during seismic sequences, the computation of the magnitude of completeness is crucial to obtain an unbiased *b*-value estimation and to avoid non-physical fluctuation of this parameter (Lombardi, 2021).

Another future improvement of our methodology can be the application of the weighted likelihood estimation to the parameters of the tapered version of Gutenberg-Richter law (Kagan, 2002).

CONCLUSIONS

The results of this work can be summarized in three main points:

1) we developed a method to estimate the spatial variation of the Gutenberg-Richter *b*-value and its uncertainty for catalogs with a time-varying magnitude of completeness, using the maximum weighted likelihood approach;

2) we presented a simple approach to show on a map the candidate *b*-values which may be different from the overall value;

3) we suggested a method to compare the performances of two different models for spatial b-value estimation (in our case the model based on the weighted likelihood estimation and the uniform model) using the Bayes factor.

We finally applied our method to the new Italian instrumental seismic catalog, showing that the model with a spatial-varying *b*-value is significantly better than the model with a uniform *b*-value; this result is similar to the one obtained by Hiemer and Kamer (2016) for California.

Thanks to the flexibility of the weighted likelihood approach, our method can be easily adapted to different spatial kernels, or different types of smoothing distances (e.g. the adaptive smoothing distance, Helmstetter et al., 2007).

DATA AND RESOURCES

The catalog used in this work is described in Lolli et al. (2020), and available at: http://horus.bo.ingv.it/ (last access September 2020).

In the Supplemental Material are presented other b-value spatial maps for different smoothing distances and for a conservative magnitude of completeness.

The code for the spatial b-value mapping is freely available at: https://github.com/MatteoTaroniINGV

ACKNOWLEDGMENTS

We thank the Associate Editor and the reviewers (Maura Murru and Martijn van den Ende) for their suggestions, which allow us to improve the paper. This study was partially supported by the “Real-time Earthquake Risk Reduction for a Resilient Europe” (RISE) project, funded by the European Union’s Horizon 2020 research and innovation program (Grant Agreement Number 821115). JZ is also partially supported by China Earthquake Science Experiment Project, China Earthquake Administration (CEA; Grant Numbers2019CSES0105 and 2019CSES0106).

REFERENCES

Ahmed, E. S., Volodin, A. I., and A. A. Hussein (2005). Robust weighted likelihood estimation of exponential parameters, *IEEE Trans. Reliab.* **54**(3) 389-395.

Aki, K. (1965). Maximum likelihood estimate of b in the formula logN=a-bM and its confidence limits, *Bull. Earthq. Res. Inst. (Tokyo)* **43** 237–239.

Bender, B. (1983). Maximum likelihood estimation of b-values for magnitude grouped data, *Bull. Seism. Soc. Am.* **73**(3) 831–851.

Castellaro, S., Mulargia, F., and Y. Y. Kagan (2006). Regression problems for magnitudes, *Geophys. J. Int.* **165**(3) 913–930.

Della Vedova, B., Bellani, S., Pellis, G., and P. Squarci (2001). Deep temperatures and surface heat flow distribution, in *Anatomy of an orogen: the Apennines and adjacent Mediterranean basins*, Springer, Dordrecht, 65-76.

Dorfman, R. (1938). A Note on the δ-Method for Finding Variance Formulae, *Biometrics Bull.* **1** 129–137.

Frankel, A. (1995). Mapping seismic hazard in the central and eastern United States, *Seism. Res. Lett.* **66**(4), 8-21.

Gulia, L., and S. Wiemer (2010). The influence of tectonic regimes on the earthquake size distribution: A case study for Italy, *Geophys. Res. Lett*. **37** L10305.

Gulia, L., Rinaldi, A. P., Tormann, T., Vannucci, G., Enescu, B., and S. Wiemer (2018). The effect of a mainshock on the size distribution of the aftershocks, *Geophys. Res. Lett*. **45**(24) 13-277.

Gutenberg, B., and C. F. Richter (1944). Frequency of earthquakes in California, *Bull. Seism. Soc. Am.* **34**(8) 185–188.

Helmstetter, A., Kagan, Y. Y., and D. D. Jackson (2007). High-resolution time-independent grid-based forecast for M≥ 5 earthquakes in California, *Seism. Res. Lett.* **78**(1) 78-86.

Herrmann, M., and W. Marzocchi (2021). Inconsistencies and Lurking Pitfalls in the Magnitude–Frequency Distribution of High-Resolution Earthquake Catalogs, *Seism. Res. Lett.* doi: 10.1785/0220200337

Hiemer, S., and Y. Kamer (2016). Improved seismicity forecast with spatially varying magnitude distribution, *Seism. Res. Lett.* **87**(2A) 327-336.

Hu, F., and J. V. Zidek (2002). The weighted likelihood, *Can. J. Stat.* **30**(3) 347-371.

Kagan, Y. Y., and D. D. Jackson (2000). Probabilistic forecasting of earthquakes, *Geophys. J. Int.* **143**(2) 438-453.

Kagan, Y.Y. (2002). Seismic moment distribution revisited: I. Statistical results, *Geophys. J. Int*. **148**(3) 520–541.

Kagan, Y. Y. (2004). Short-term properties of earthquake catalogs and models of earthquake source, *Bull. Seismol. Soc. Am.* **94**(4) 1207-1228.

Kass, R. E., and A. E. Raftery (1995). Bayes factors, *J. Am. Stat. Assoc.* **90**(430) 773-795.

Kamer, Y., and S. Hiemer (2015). Data-driven spatial b value estimation with applications to California seismicity: To b or not to b, *J. Geophys. Res. Solid Earth* **120**(7) 5191-5214.

Lolli, B., and P. Gasperini (2006). Comparing different models of aftershock rate decay: The role of catalog incompleteness in the first times after main shock, *Tectonophysics* **423**(1-4) 43-59.

Lolli, B., Randazzo, D., Vannucci, G., and P. Gasperini (2020). HOmogenized instRUmental Seismic catalog (HORUS) of Italy from 1960 to present, *Seism. Res. Lett.* **91**(6) 3208-3222.

Lombardi, A.M.(2021). A Normalized Distance Test for co-determining the completeness magnitude and b-value of earthquake catalogs, *J. Geophys. Res. Solid Earth* e2020JB021242.

Marzocchi, W., and L. Sandri (2003). A review and new insights on the estimation of the b-value and its uncertainty, *Ann. Geophys,* **46** 1271–1282.

Marzocchi, W., Spassiani, I., Stallone, A. and M. Taroni (2020). How to be fooled searching for significant variations of the b-value, *Geophys. J. Int.* **220**(3), 1845-1856.

Marzocchi, W., Zechar, J. D., and T. H. Jordan (2012). Bayesian forecast evaluation and ensemble earthquake forecasting, *Bull. Seismol. Soc. Am.* **102**(6), 2574-2584.

Meletti, C., Galadini, F., Valensise, G., Stucchi, M., Basili, R., Barba, S., Vannucci, G., and E. Boschi (2008). A seismic source zone model for the seismic hazard assessment of the Italian territory, *Tectonophysics* **450**(1-4), 85-108.

Murru, M., Taroni, M., Akinci, A.,and G. Falcone (2016). What is the impact of the August 24, 2016 Amatrice earthquake on the seismic hazard assessment in central Italy? *Ann. Geophys.* **59**(5) doi: 10.4401/ag-7209.

Ogata, Y. & Yamashina, K., 1986. Unbiased estimate for b-value of magnitude frequency, *J. Phys. Earth*, **34,** 187–194.

Scholz, C. H. (1968). The frequency magnitude relation of microfracturing in rock and its relation to earthquakes, *Bull. Seismol. Soc. Am.* **58**(1) 399−415.

Schorlemmer, D., Wiemer, S., and M. Wyss (2004). Earthquake statistics at Parkfield: 1. Stationarity of b values, *J. Geophys Res. Solid Earth* **109** B12307.

Schorlemmer, D., Wiemer, S. and M. Wyss (2005). Variations in earthquake-size distribution across different stress regimes, *Nature* **437** 539–542.

Schorlemmer, D., Mele, F., and W. Marzocchi (2010). A completeness analysis of the National Seismic Network of Italy, *J. Geophys Res. Solid Earth* **115** B4.

Taroni, M. (2021). Back to the future: old methods for new estimation and test of the Gutenberg–Richter b-value for catalogues with variable completeness, *Geophys. J. Int.* **224**(1) 337-339.

Tormann, T., Wiemer, S., and A. Mignan (2014). Systematic survey of high-resolution b value imaging along Californian faults: Inference on asperities, *J. Geophys Res. Solid Earth* **119**(3) 2029-2054.

Tormann, T., Enescu, B., Woessner, J., ans S. Wiemer (2015). Randomness of megathrust earthquakes implied by rapid stress recovery after the Japan earthquake, *Nat. Geosci.* **8**(2) 152-158.

Utsu, T. (1966). A statistical significance test of the difference in b-value between two earthquake groups, *J. Phys. Earth* **14**(2), 37–40.

Warren, N. W., and G. V. Latham (1970). An experimental study of thermally induced microfracturing and its relation to volcanic seismicity, *J. Geophys Res.***75**(23), 4455-4464.

Zhuang, J. (2015). Weighted likelihood estimators for point processes, *Spat. Stat.* **14** 166-178.

Full mailing address for each author:

Matteo Taroni: Via di Vigna Murata 605, 00143, Rome, RM, Italy; email: matteo.taroni@ingv.it

Jiancang Zhuang: 10-3 Midori-cho, Tachikawa, Tokyo, 190-8562, Japan; email: zhuangjc@ism.ac.jp

Warner Marzocchi: Via Vicinale Cupa Cintia, 21, 80126, Napoli, Italy; email: warner.marzocchi@unina.it

Tables:

Table 1: Completeness magnitude of the catalog, with the starting date for each level of completeness.

Starting date	Completeness magnitude (Mw)
1960-1-1	4.0

1981-1-1	3.0
1990-1-1	2.5
2003-1-1	2.1
2005-4-16	1.8

List of figure captions:

Figure 1: the black dots represent the epicenters of the events used in this study, the grey polygon borders the zone of investigation for the *b*-value mapping.

Figure 2: Panel (a): *b*-value map; panel (b): standard deviation map; panel (c): a map for the *b*-values that are significantly differents from the one of the whole catalog. These maps refer to a smoothing distance of 30 km. This figure will appear in color only in the online version, not in the printed version.

Figure 3: Panel (a): Bayes factor (in a log scale) of the model with a spatial-varying *b*-value against the model with a uniform b-value as a function of time, for the testing dataset (2010-1-1 – 2019-12-31). The black curve is the computation for a testing dataset from Mw 1.8+, the grey curve for Mw 2.1+, and the light grey for Mw 2.4+; the black dashed line represents the very strong evidence line of the Bayes factor; panel (b): the daily number of events with Mw 1.8+.

Figures:

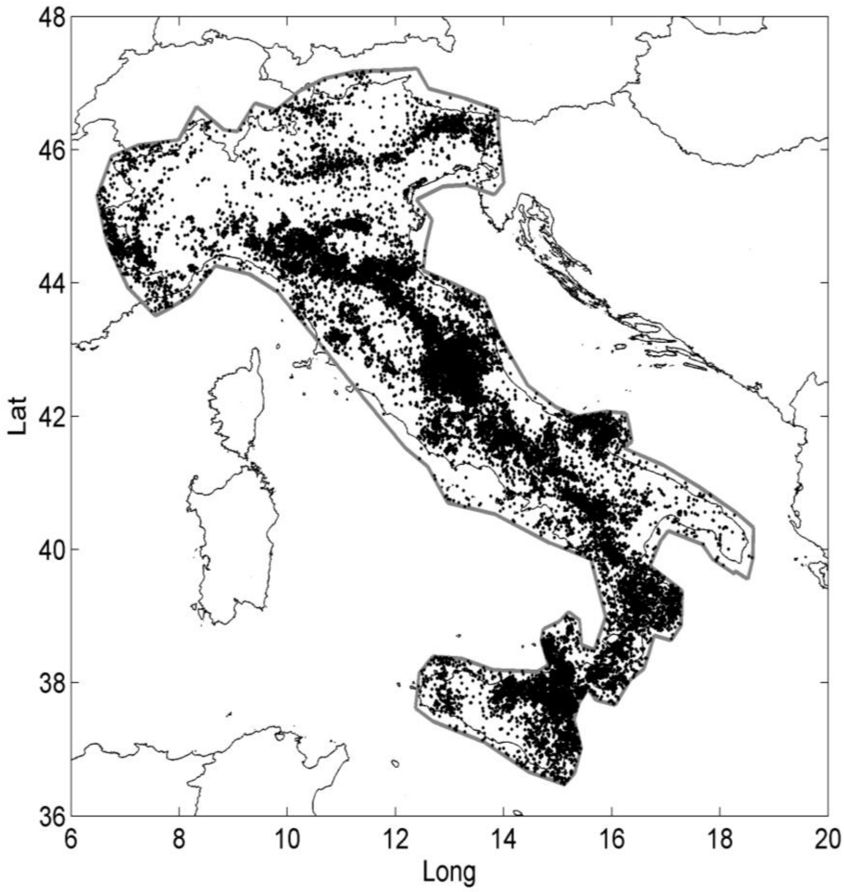

Figure 1: the black dots represent the epicenters of the events used in this study, the grey polygon borders the zone of investigation for the *b*-value mapping.

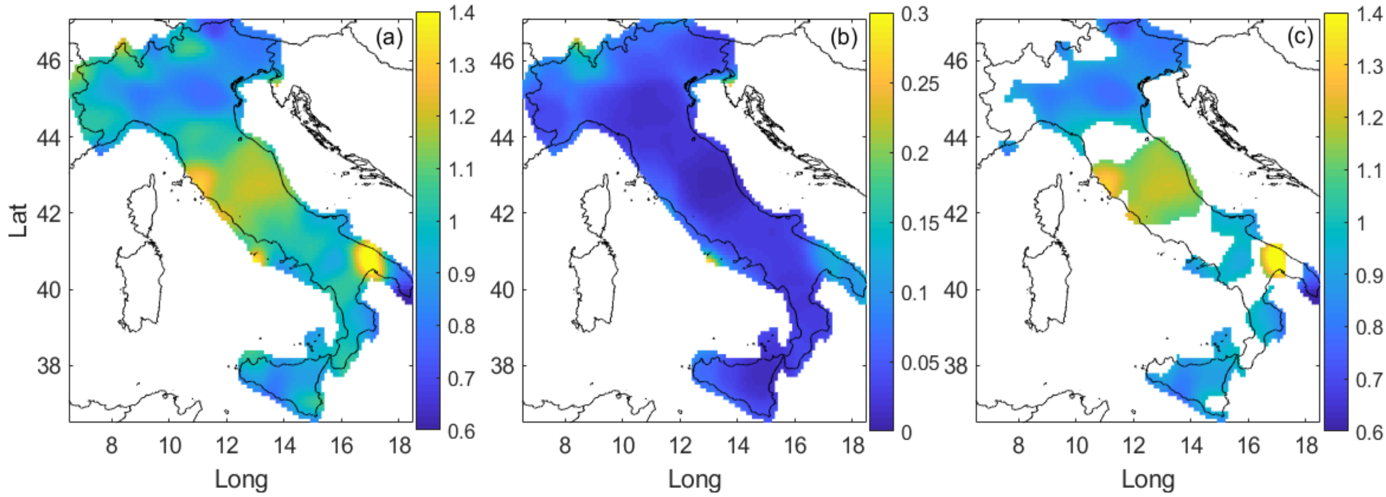

Figure 2: Panel (a): *b*-value map; panel (b): standard deviation map; panel (c): a map for the *b*-values that are significantly different from the one of the whole catalog. These maps refer to a smoothing distance of 30 km. This figure will appear in color only in the online version, not in the printed version.

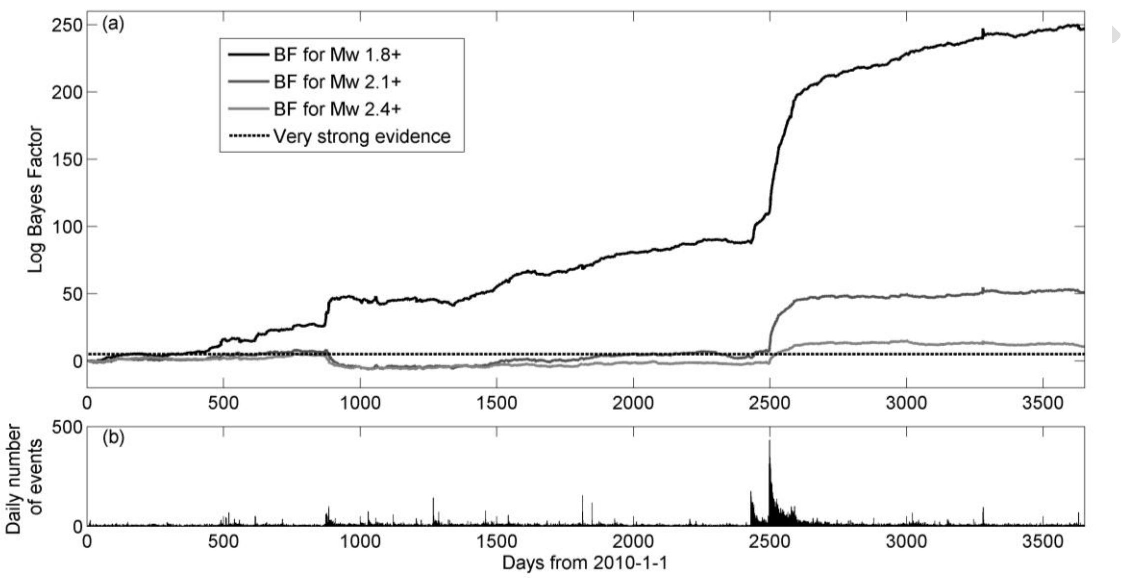

Figure 3: Panel (a): Bayes factor (in a log scale) of the model with a spatial-varying *b*-value against the model with a uniform b-value as a function of time, for the testing dataset (2010-1-1 – 2019-12-31). The black curve is the computation for a testing dataset from Mw 1.8+, the grey curve for Mw 2.1+, and the light grey for Mw 2.4+; the black dashed line represents the very strong evidence line of the Bayes factor; panel (b): the daily number of events with Mw 1.8+.

APPENDICES

A) Derivation of the weighted maximum likelihood estimator for the *b*-value

If we set $\beta = \ln(10)\, b$ and $X_i = M_i - M_{min}^{(k)}$, the Gutenberg-Richter law reads as the exponential distribution with rate parameter β (Aki, 1965; Taroni, 2021). The log-likelihoods for MLE (LL) and weighted MLE (WLL) (Hu and Zidek, 2002; Ahmed et al., 2005) are:

$$LL = \sum_{i=1}^{N} \ln f(X_i) \qquad (A1)$$

$$WLL = \sum_{i=1}^{N} W_i \ln f(X_i) \qquad (A2)$$

where $f(x) = \beta e^{-\beta x}$ is the probability density function of the exponential distribution.

From the conditions $\frac{\partial LL}{\partial \beta} = 0$ and $\frac{\partial WLL}{\partial \beta} = 0$, and considering that the sum of all the W_i is 1, we obtain:

$$-\sum_{i=1}^{N} X_i + \frac{N}{\beta} = 0 \qquad (A3)$$

$$-\sum_{i=1}^{N} W_i X_i + \frac{1}{\beta} = 0 \qquad (A4)$$

From these equations we obtain the final MLE and weighted MLE for β:

$$\hat{\beta} = \frac{N}{\sum_{i=1}^{N} X_i} \qquad (A5)$$

$$\hat{\beta} = \frac{1}{\sum_{i=1}^{N} W_i X_i} \qquad (A6)$$

B) Derivation of the weighted maximum likelihood estimator for standard error of the *b*-value

The Delta method (Dorfman, 1938) is in fact the law of error propagation. It asserts that if $Y \sim Norm(\mu, \sigma^2)$ asymptotically, then $f(Y) \sim Norm(f(\mu), [f'(\mu)]^2\sigma^2)$ asymptotically, where $Norm$ is the Gaussian normal distribution.

The expected value and the variance of X_i (that follows an exponential distribution) can be computed with the equations:

$$E(X_i) = \frac{1}{\beta} \qquad (B1)$$

$$Var(X_i) = \frac{1}{\beta^2} \qquad (B2)$$

Then, the expected value and the variance of $Y \stackrel{\text{def}}{=} \sum_{i=1}^{N} W_i X_i$ will be:

$$E(Y) = \frac{1}{\beta} \qquad (B3)$$

$$Var(Y) = \frac{\sum_{i=1}^{N} W_i^2}{\beta^2} \qquad (B4)$$

If N is large enough (we verify through simulations that N must be at least 10^3)), then $Y \sim Norm\left(\frac{1}{\beta}, \frac{\sum_{i=1}^{N} W_i^2}{\beta^2}\right)$.

Since $\hat{\beta} = \frac{1}{\sum_{i=1}^{N} W_i X_i} = \frac{1}{Y}$ (eq. A6), if we apply the Delta method with $f(x) = \frac{1}{x}$, we obtain:

$$\hat{\beta} = \frac{1}{Y} \sim Norm\left(\beta, \beta^2 \sum_{i-1}^{N} W_i^2\right) \qquad (B5)$$

And finally:

$$\sigma_{\hat{\beta}} = \beta \sqrt{\sum_{i=1}^{N} W_i^2} \qquad (B4)$$